Contrib Mineral Petrol (2005) 149: 98–112
DOI 10.1007/s00410-004-0639-2

ORIGINAL PAPER

Glen S. Wallace · George W. Bergantz

Reconciling heterogeneity in crystal zoning data: An application of shared characteristic diagrams at Chaos Crags, Lassen Volcanic Center, California

Received: 29 March 2004 / Accepted: 8 November 2004 / Published online: 4 December 2004

Abstract Isotope, trace element, and textural crystal zoning patterns record heterogeneity in magmatic systems not resolved by whole rock analyses. These zoning data are used to infer crystal residence times, magma mixing, and other magmatic processes in many magmatic systems. We present the shared characteristic diagram (SCD) as an organizational framework for crystal zoning data that compares information from different phases and chemical tracers in a common framework. An example from Chaos Crags in the Cascade arc, produces three main results. (1) Anorthite zoning profiles in plagioclase have fewer shared characteristics in mafic inclusions than in the host rhyodacite. (2) Single-crystal $^{87}Sr/^{86}Sr$ data from previous studies (Tepley et al. 1999) are consistent with more shared history between crystals than in anorthite profiles. This difference reflects a more homogeneous distribution of $^{87}Sr/^{86}Sr$ than the intensive parameters controlling plagioclase composition. (3) The Chaos Crags system exhibits a layer of heterogeneity in crystal populations that is not represented in whole-rock analyses that indicate only simple binary mixing. The inconsistency between $^{87}Sr/^{86}Sr$ and anorthite zoning data highlights decoupling between compositionally controlled and temperature/water-controlled zoning in plagioclase from Chaos Crags.

Introduction

Compositional zoning profiles in crystals have long been recognized as a key to interpreting physiochemical processes in upper crustal reservoirs (Vance 1962). Crystals are particularly useful as indicators of magmatic processes because they both record chemical conditions and act as physical objects (Fig. 1). This is an important distinction from the melt phase, which cannot preserve a structured record of previous environmental conditions. Additionally, the "stratigraphy" preserved in zoning profiles provides chronological ordering for processes recorded in crystal textures and chemical variations. Identification of crystal populations with similar zoning characteristics thus provides the opportunity to mutually constrain the physical and chemical evolution of magmatic systems (Izbekov et al. 2002; Wallace and Bergantz 2002). Early study of plagioclase anorthite profiles from plutonic and volcanic rocks showed variable degrees of similarity, interpreted as differences in the heterogeneity of the crystal growth environments or transient changes in magmatic environments (Greenwood and McTaggert 1957; Anderson 1983). Micro-analytical advances have revealed a scale of heterogeneity in which REE and isotopic characteristics vary between and within individual crystals (Davidson and Tepley 1997; Tepley et al. 1999, 2000; Davidson et al. 2001; Vazquez and Reid 2001, 2002).

Many studies exploit the information content of crystal populations to infer magma mixing and transient changes in intensive variables in magmatic systems. For example, glomerocrysts from the Bandelier Tuff with high $^{87}Sr/^{86}Sr$ record variable degrees of contamination from radiogenic country rocks dependent on distance from the country rock contact (Wolff et al. 1999). Differences in the Sr concentration of plagioclase from the eruption of Mt Mazama record gathering of crystals from high- and low-Sr magma reservoirs (Bacon and Druitt 1988; Druitt and Bacon 1989). In the Pleasant Bay intrusion, plagioclase phenocrysts are in isotopic disequilibria with enveloping mafic magma, but in equilibrium with the bulk granite indicating crystal transfer during intrusion of the mafic magma (Waight et al. 2001). Plagioclase in andesites from Soufriere Hills, Montserrat, reflect mixing of crystal populations in a thermally het-

Editorial Responsibility: K. Hodges

G. S. Wallace · G. W. Bergantz (✉)
Department of Earth and Space Sciences,
University of Washington, Box 351310,
Seattle, WA 98195-1310, USA
E-mail: bergantz@u.washington.edu
Tel.: +1-206-6854972
Fax: +1-206-5430489

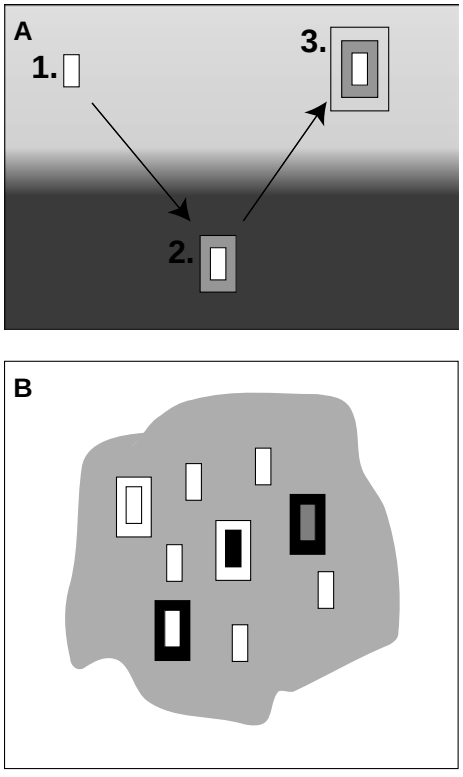

Fig. 1 The culmination of populations of crystals with individually complex histories produces diverse crystal populations. **a** An individual crystal may experience changing thermal and compositional environments during crystallization. These changes produce sequential features in zoning profiles and a crystal-stratigraphic record of the transport path of the crystal. **b** Zoned crystal populations record the details of the integrated characteristics averaged in whole rock analyses

erogeneous magma chamber (Murphy et al. 2000). However, while analytical methods for individual crystals provide detailed chemical information, profile alignment and data organization has remained largely subjective. The problem of profile alignment has prevented the use of statistically constrained profile comparison.

We present the shared characteristic diagram (SCD) as an organizational framework for categorizing data from zoning profiles. The SCD framework provides statistically constrained correlations between profiles in a time-stratigraphic format. SCD for geochemical tracers in specific phases are compared to infer the amount of shared history in populations of crystals. The SCD increases the utility of existing data and provide a framework to guide sample selection for expensive or time-consuming analyses.

Empirical profile alignment techniques compensate for geometric distortions in crystal zoning profiles measured from thin sections. Direct comparison of aligned zoning profiles permits quantitative comparison between crystals and diverse chemical and zoning data types (Wallace and Bergantz 2002, 2004). In our approach, computer algorithms apply parametric guidelines to profile alignment, substantially reduce selective bias, and return information on the spatial distribution shared characteristics. The distribution of shared characteristics in zoning profiles provides a proxy for shared physiochemical history in crystal populations.

We selected Chaos Crags for this study as a well-documented type locality for magma mixing (Fig. 2) (Williams 1931; Eichelberger 1980; Heiken and Eichelberger 1980; Davidson and Tepley 1997; Tepley et al. 1999). Results from SCD analyses revealed greater heterogeneity in major element zoning patterns than expected and, along with a difference in heterogeneity between anorthite and $^{87}Sr/^{86}Sr$, prompted an evaluation of differences in boundary conditions for each chemical tracer. This line of research leads us to interpret a transiently decoupled thermal and compositional evolution of the Chaos Crags magma system.

Crystal histories as recorded in zoning profiles

Compositional profiles in individual crystals reflect the often complicated interplay between crystal-melt kinetics, transient changes in the system, and subsequent effects of intracrystalline diffusion (Fig. 1) (Izbekov et al. 2002; Troll and Schmincke 2002; Costa et al. 2003). The variability of chemical tracers is controlled by changes in environmental conditions, distribution coefficients for REE, and solid solution for major elements (Blundy and Wood 2003). Different phase-tracer pairs produce unique zoning patterns when they respond differently to changes in the environment or they have contrasting histories. However, if a transient change occurs over a shorter timescale than the crystal can grow a new zone, or if a crystal is resorbed, events may not be recorded.

Shared history is inferred from the similarity of zoning profiles assuming that crystals in the same phase–tracer pairing growing in the same environment preserve the same zoning pattern. Minerals with solid solution exhibit two types of compositional zoning reflecting both kinetics and environmental changes. Feedback between crystal growth rate and diffusion in a boundary layer of melt around the crystal produces small compositional variations in zoning profiles referred to as oscillatory zoning (Bottinga et al. 1966; Allegre and Jaupart 1981; Pearce 1994; Lheureux and Fowler 1996; Fowler et al. 2002). Changes in the local environment can produce larger, more distinct spikes and plateaus in zoning profiles—the features of interest for most SCD applications. The expression of these zoning types is dependent on the sensitivity of each phase to changing local conditions. Oscillatory, or Type I, zoning in plagioclase is characterized by 1–3% changes in anorthite content over lengths scales of 1–100 μm (Pearce and Kolisnik 1990). Type II zoning in plagioclase reflects changes in the local environment of the crystals and is characterized by variations $>4\%$ anorthite over widths >50 μm. The identification of phase–tracer populations

allows evaluation of the relative heterogeneity of chemical tracers in magmatic systems.

Isotopic variations in crystal populations provide a unique constraint on crystal histories because isotopes of the same element do not fractionate during crystal growth. Isotopic values provide an index of crystal histories independent of pressure and temperature. Mixing and mingling in a heterogeneous environment produces variations in zoning patterns that are a direct reflection of the isotopic composition of their host environment. $^{87}Sr/^{86}Sr_I$variations in crystal populations have been used to document crystal transfer in plutonic and volcanic suites where end-member bulk rock compositions match crystal variations (Davidson and Tepley 1997; Tepley et al. 1999; Waight et al. 2000, 2001).

Differences between zoning profiles are produced by juxtaposition of crystals with differing magmatic histories as well as localized transient changes in the magma chamber environment. Transient changes produce localized crystal populations along thermal or compositional gradients. Gathering of crystals in a common volume by a variety of processes produces crystal populations with similar rims and dissimilar cores that retain the chemical signature of the previous environments. In either case, the transition from similar rims to dissimilar cores marks the point at which crystals came into a common environment. This provides a basis for organizing compositional profiles into regions with and without shared characteristics. Intensive parameters such as temperature and pH_2O may vary independently of compositional tracers of magma or crystal sources. For example, changes in temperature will affect major element compositions and crystal growth rates, but will not affect the isotopic characteristics of growing crystals. Additionally, environmental changes may produce different zoning profiles in other mineral phases due to differences in the kinetics of crystal growth and dissolution. In the next section, we present the SCD framework to organize and assess zoning data from one or more chemical tracers and assess heterogeneity in crystal populations.

Shared characteristic diagrams

An SCD is a graphical representation of the distribution of correlative zoning patterns in a population of zoning profiles (Fig. 3) (Wallace and Bergantz 2002). Shared characteristics are defined as segments of zoning profiles with similar chemical values or patterns at the same position in each profile. The specific criteria for defining a shared characteristic are dependent on phase–tracer pair profile variance, resolution, and uncertainty. The essential elements of an SCD are the decorrelation point, an interval of shared characteristics between the rim and decorrelation point, and an interval of non-correlative characteristics between the decorrelation point and the apparent core of the crystal. The decorrelation point is determined for each pair of profiles and marks the first point between the rim and core at which characteristics are no longer significantly similar between a pair of

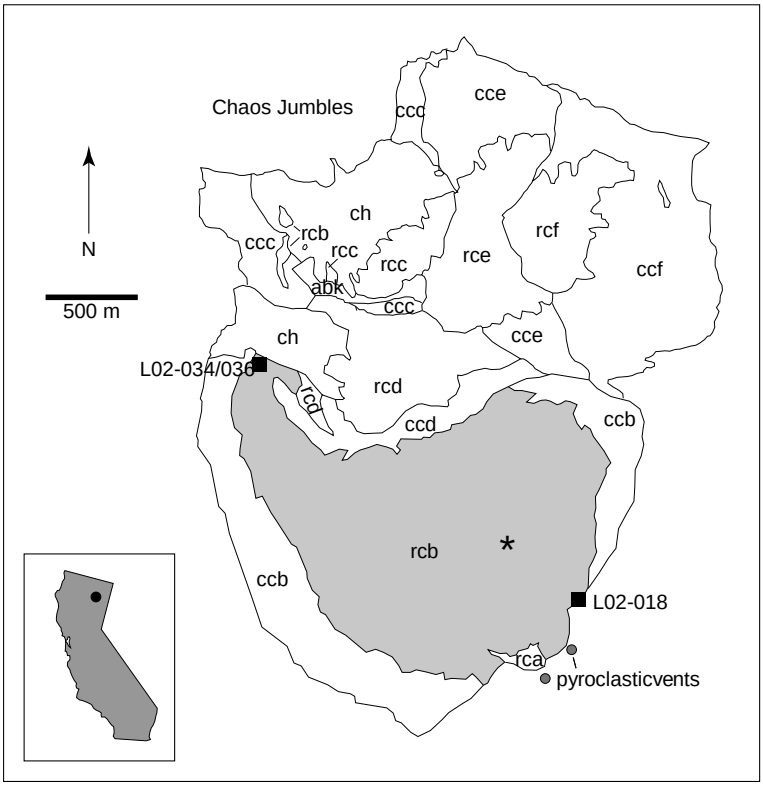

Fig. 2 Geologic map of Chaos Crags modified from Christiansen et al. (2003) with sample locations. Chaos Crags is located in northern California at the southern end of the Cascade Arc, as indicated by *black dot* in inset. Sample locations are marked by *black squares*. Units in chronological order are: *abk* andesite of Brokeoff Volcano, *rca* rhyodacite dome A, *rcb* rhyodacite dome B, *ccb* talus from dome B, *rcc* rhyodacite dome C, *ccc* talus from dome C, *rcd* rhyodacite dome D, *ccd* talus from dome D, *rce* rhyodacite dome E, *cce* talus from dome E, *rcf* rhyodacite dome F, and *ccf* talus from dome F, *ch* undifferentiated talus. Note that talus and dome units have been grouped in places for clarity. *Gray circles* at south end of Chaos Crags mark the centers of the tephra rings. Pyroclastic deposits are not shown on map. The *star symbol* in dome B marks the mapped vent location

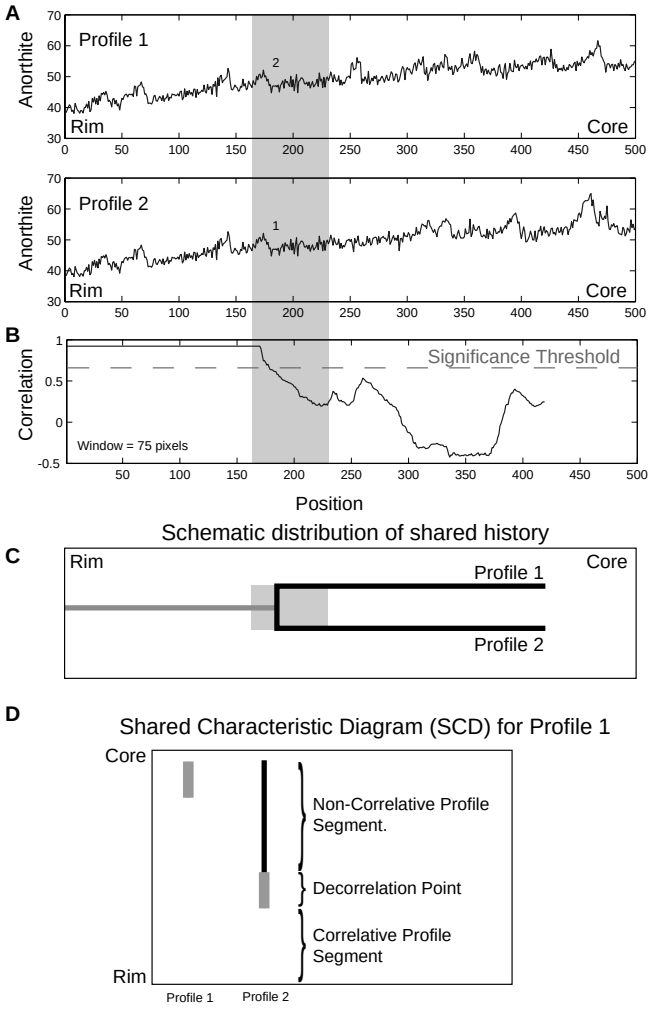

Fig. 3 Generation of a shared characteristic diagram (SCD) from two artificial plagioclase zoning profiles. Cross-correlation profiles are determined by calculating the correlation coefficient in a sliding window and plotting the values as a function of window position. The window width is selected to be wider than the features of interest. For example, if spikes 30 points wide are of interest, a window 40–50 points wide should be selected for the analysis. Decorrelation points are the point at which cross-correlation values between a pair of profiles drops below the significance threshold. Significance levels for profile correlation are determined using Monte Carlo routines (Wallace and Bergantz 2004). SCD plots are generated by locating the decorrelation point between sets of profiles. SCD output from each cross-correlation produce three segments: (1) a correlative segment representing an interval of shared history; (2) the location of the decorrelation point with spatial uncertainty determined by the correlation window width; and (3) a non-correlative segment of the zoning profile representing the non-shared characteristics and history. Profile alignment and alignment quality indicators for these profiles are shown in Fig. 5. The tick marks indicate the maximum interval of shared characteristics

profiles. The position of the decorrelation point is the primary indicator of profile similarity.

SCD are constructed in three steps (Fig. 3). (1) Correlation coefficients are calculated in a window that is moved along the length of the profiles from rim to core. This generates a cross-correlation profile. The window width is selected to overlap the widest type II zoning change; either spike width or plateau edge. (2) Correlative segments are identified by applying a significance threshold to the cross-correlation profile. Correlation values below the significance threshold indicate the position of non-shared characteristics. (3) The point closest to the rim at which the cross-correlation value is below the significance threshold is the decorrelation point for the profile pair. Significance levels for cross-correlation profiles are determined using a Monte Carlo routine (Wallace and Bergantz 2004). The Monte Carlo routine used for SCD is slightly different than the routine used for wavelet-based correlation (WBC). In both techniques, reference distributions are based on the correlation of numerically generated synthetic zoning profiles with randomly distributed zoning characteristics. For the SCD routine, a windowed correlation is calculated along each profile; the entire profile length is correlated in WBC. Thus, each pair of profiles will generate a number of correlation coefficients equal to the length of the synthetic profiles minus the window width. Sets of 15–20 synthetic profiles in Monte Carlo experiments produce between 95,000 and 170,000 correlation coefficients and provide consistent reference distributions for the determination of significance levels. Reference distributions from the Monte Carlo experiments are often skewed with non-zero means because zoning profiles have similarly shaped peaks and the measured values are not random series of numbers. This reinforces the caution against using traditional reference distributions to determine significance levels for the correlation of zoning profiles.

The distribution of decorrelation points in SCD reflects the minimum heterogeneity of the magmatic environment (Fig. 4). Homogeneous environments produce crystal populations with decorrelation points near the core reflecting their shared history. Heterogeneous environments produce crystal populations with little shared history, and decorrelation points near the rims of crystals. When chemical tracers are decoupled in space, they will produce different SCD in the same set of crystals. The net shared characteristics for the tracers reflect the relative heterogeneity. Chemical tracers that are decoupled in space produce different SCD that can be used to rank their relative heterogeneity. If the distribution of decorrelation points is similar, then the degree of heterogeneity is similar. Decorrelation points nearer the core indicate a more homogeneous distribution. Thus, SCD can constrain what variables are changing in a system. If a tracer sensitive to composition, pressure, and temperature produces an SCD with more shared history than another tracer that is sensitive only to melt composition, composition is more heterogeneous than pressure or temperature in the system. $^{87}Sr/^{86}Sr$ variations in compositionally homogeneous plagioclase from the Columbia River Basalt Group are consistent with this type of interpretation (Tollstrup et al. 2002).

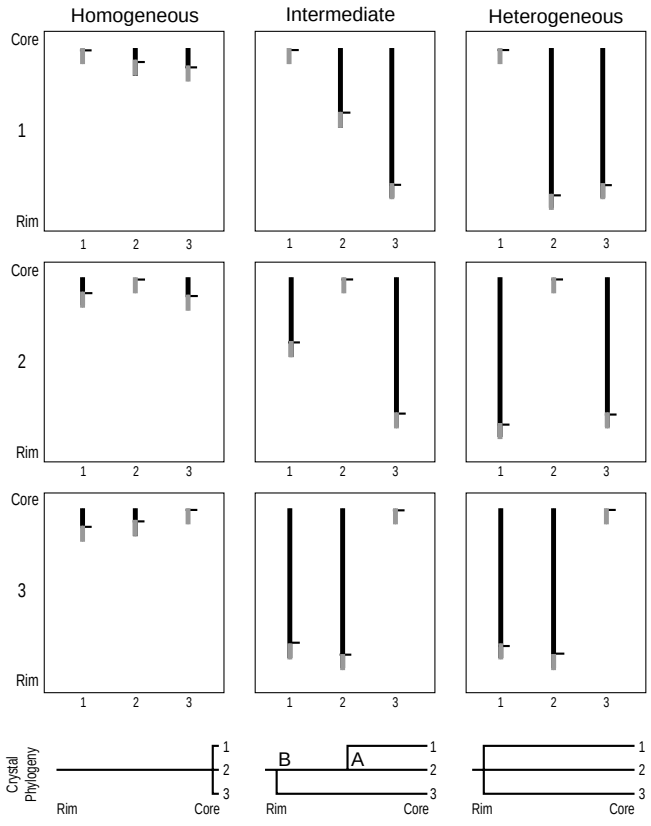

Fig. 4 Comparison of hypothetical shared characteristic diagrams (SCD) illustrating correlation patterns associated with heterogeneous, intermediate, and homogeneous crystal populations. *Gray bars* indicate the location and spatial uncertainty in the location of the decorrelation point. Each row of SCD plots is in the reference frame of the profile number at the left end of the row. For example, all SCD in the middle row are in the reference frame of profile 2. For example, all plots of profile 2 in the middle row correlate all of the way to the core because profile 2 will always correlate perfectly against itself. *Black line segments* indicate non-correlative segments of zoning profiles. All profiles are the same length in this figure for clarity. Regions between the rim and decorrelation point correlate above the significance threshold (as in Fig. 3). Crystal phylogeny show the schematic evolution of the crystal population shown in the corresponding column of SCD plots. For the homogeneous population, crystals have shared growth histories from the rim to the core. For the intermediate population, profiles 1 and 2 correlate for about half of their length, consistent with the top two SCD plots. Profile 3 decorrelates against profiles 1 and 2 near the rim in the bottom SCD. For the heterogeneous population, decorrelation points are consistently near the rim and profiles have little shared history in the corresponding crystal phylogeny. At point A, profiles 1 and 2 begin growing matching zoning profiles interpreted as the point at which they enter a common environment, but not the same as profile 3. At point B profile 3 begins growing a zoning profile matching profiles 1 and 2 and all three profiles are interpreted to be in the same environment

Profile normalization

Most sections through crystals in petrographic thin sections are off-center and not oriented normal to growth zones (Pearce 1984). These non-ideal orientations produce geometric distortions in measured zoning profiles. Geometric distortions reduce to truncation of information at the core in off-center crystal sections, and an evenly distributed stretching due to mis-orientation (Wallace and Bergantz 2004). Truncation of information from the core is not recoverable without re-sectioning the crystal. Stretching due to mis-orientation can be compensated for if a compensating stretching can be determined. We adopt an empirical profile normalization routine that aligns profiles to maximize the interval of shared characteristics between the rim and decorrelation point (Fig. 5). Type II zoning features in plagioclase will be offset in misaligned profiles. Misalignment will cause decorrelation points to migrate toward crystal rims. Decorrelation points will migrate toward the core as profiles are stretched into their proper alignment. Thus, the best-fit alignment is the stretching at which the decorrelation point is furthest from the rim.

For every possible pair of profiles in the data set, one profile is designated as the reference profile and one as the variable profile for profile normalization. The variable profile is duplicated and stretched over a specified range of profile interpolations producing a matrix of different lengths of the variable profile. A decorrelation point is determined for each interpolation of the variable profile relative to the reference profile. The stretching that produces a decorrelation point the farthest from the profile rim in the reference profile is selected as the best fit (Fig. 5a). For n profiles, this produces an $n \times n$ matrix of best-fit pairs. Profiles normalized to themselves lie along the diagonal, and variable-reference profile alignments fill the upper and lower triangles. Duplication of profile normalization above and below the diagonal provides a check for internal consistency where equivalent pairs are expected to produce reciprocal best-fit alignments. For example, if a best-fit stretching of 2.0 is determined for pairing n_{ij}, then 0.5 is expected for n_{ji} within alignment error. Profile alignment error is affected by correlation window width and position of the decorrelation point. Alignment error decreases away from the rim as the correlation window becomes a smaller fraction of the correlative segment of the profile. This normalization approach selects for the most possible shared characteristics in a profile pair, but does not assume shared history. This introduces a systematic bias of the decorrelation point toward the core because it is statistically possible for unrelated profiles to have similar characteristics. It is also possible to miss the true best fit and bias decorrelation point locations toward the rim if the step size between interpolated lengths is too large. Step size is confirmed in plots of decorrelation position vs interpolated length.

A computer algorithm for SCD analysis and profile normalization in MATLAB R12 is available from the corresponding author.

Application to Chaos Crags, Lassen Volcanic Center, California

Chaos Crags is a type locality for mixing of rhyodacite and basaltic andesite in the Cascade Arc (Fig. 2) (Wil-

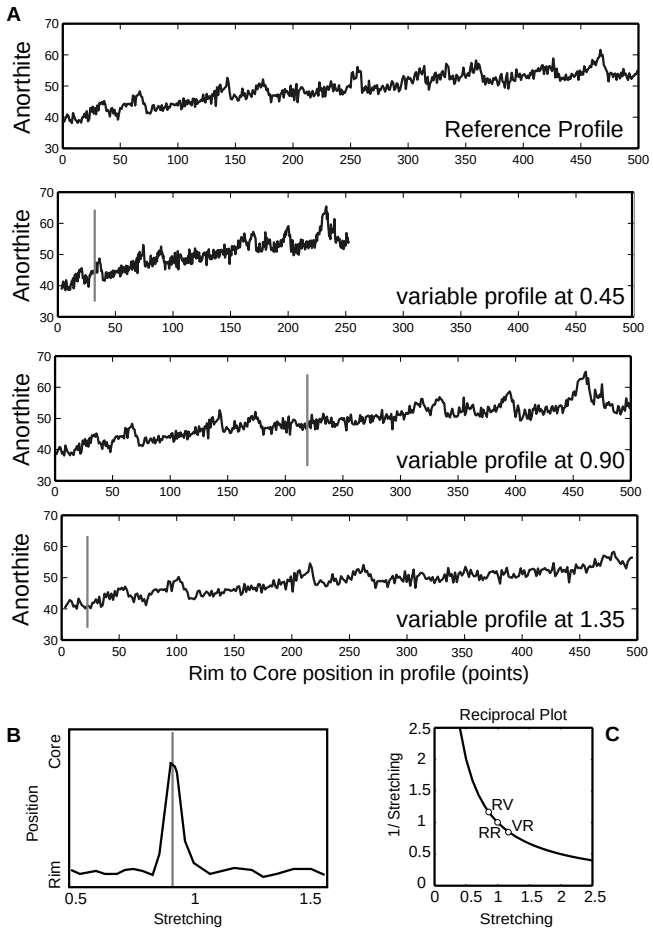

Fig. 5 Empirical protocol for profile alignment. Profiles are linearly interpolated to a range of lengths to find the best-fit alignment. **a** First, profiles are classified as the reference and variable profile. The length of the reference profile remains fixed. The length of the variable profile is stretched over a specified range as discussed in text. A decorrelation point is determined for each length of the variable profile. The combination that produces a decorrelation point closest to the core of the reference profile is selected as the best fit. **b** Plot of the fractional position of the decorrelation point against the variable profile stretching. The *gray line* marks the position of the best fit. The height of the peak relative to the standard deviation of the decorrelation point provides a measure of the quality of the alignment, as discussed in text. The quality of the fit is calculated as the peak height divided by the standard deviation. A peak with several points at the top in the position vs stretching plot indicates adequate step-size resolution. **c** Reciprocal plot of profile alignments. Point RR is the reference profile plotted against itself. Points RV and VR are the reference and variable profiles aligned against each other for each classification. Note that points are symmetrical about a line slope of one as each possible profile pairing is plotted twice

liams 1928, 1931; Eichelberger 1980; Heiken and Eichelberger 1980; Davidson and Tepley 1997; Tepley et al. 1999). Chaos Crags is one of many dacite dome clusters that make up the larger Lassen Volcanic Center (LVC) (Christiansen et al. 2002). LVC is the southernmost active volcanic center in the Cascade Arc. Lavas erupted in the LVC are bimodal and dominated by andesitic to dacitic compositions with minor basaltic andesite. Lavas erupted in the arc axis north and south of the LVC and off-axis form basaltic to andesitic cinder cones, lava cones, and small shield volcanoes. At Chaos Crags, a cluster of six rhyodacite domes totaling ~1.25 km^3 were effusively erupted beginning 1,103+/−13 y.b.p. (Clynne et al. 2002). The term rhyodacite is used to describe a range of compositions in the host magmas spanning the rhyolite–dacite compositional boundary following the convention of Clynne for the 1915 eruption of Lassen Peak (Clynne 1999). The eruption began with the emplacement of a thin tephra fall, tuff cone, and two pumiceous pyroclastic flows (Clynne et al. 2002). Dome A was then effusively erupted into the tuff cone and subsequently disrupted by an explosive eruption producing another pyroclastic flow. Formation of a second tuff cone was followed by emplacement of domes B through F. Dome B is the largest of the domes and was probably erupted after the formation of the second tuff cone without a significant hiatus (Christiansen et al. 2002; Clynne et al. 2002).

The phenocryst assemblage, groundmass texture, inclusion suite, and bulk rock chemistry of the Chaos Crags rocks form a near continuum that can be divided into two end-member groups (Clynne et al. 2002; Tepley et al. 1999). Group I includes all erupted units through dome B, while Group II includes domes C through F. Group I lavas have a glassy groundmass, contain 1–5% mafic inclusions, and have fewer reacted phenocrysts and calcic microphenocrysts than Group II lavas. Group II lavas have up to 20% mafic inclusions by volume, are devitrified and have a larger proportion of reacted phenocrysts than Group I rocks.

Disequilibrium textures and zoning patterns in both host and inclusion crystal assemblages provide compelling evidence for crystal transfer between thermally and compositionally distinct magmas. The petrographic details are well documented in the literature discussing Chaos Crags and the similar 1914–1921 Lassen Peak eruptive products and are summarized briefly here as they relate to crystal transfer (Clynne 1999; Heiken and Eichelberger 1980; Tepley et al. 1999). Plagioclase exhibits a diverse range of textures including: large complexly to weakly zoned sodic phenocrysts, some with calcic cores or strongly zoned calcic overgrowth rims; weakly zoned calcic phenocrysts; weakly zoned sodic microphenocrysts; and strongly zoned acicular calcic microphenocrysts. The calcic compositions are inferred to have grown in a mafic magma while the sodic compositions grew from a rhyodacitic melt. The presence of embayed and reacted quartz, sodic sieve-textured plagioclase phenocrysts with calcic overgrowth rims matching the composition of microphenocrysts, and hornblende in mafic inclusions is interpreted as crystal transfer from the host rhyodacite (Tsuchiyama 1985). Calcic plagioclase microphenocrysts, and sparse reacted olivine and pyroxene in the host rhyodacite support crystal transfer into the host rhyodacite.

Tepley et al. (1999) documents crystal transfer from host rhyodacite into mafic inclusions with in situ microanalysis of $^{87}Sr/^{86}Sr$ in plagioclase phenocrysts

(Tepley et al. 1999). The host rhyodacite and mafic inclusions have whole rock $^{87}Sr/^{86}Sr$ values 0.7041 and 0.7037. Phenocrysts in mafic inclusions show a consistent change from host rhyodacite to mafic $^{87}Sr/^{86}Sr$ values. Two phenocrysts from the host rhyodacite have $^{87}Sr/^{86}Sr$ values consistent with host rhyodacite whole rock values. The isotopic data set does not constrain crystal transfer from inclusion into host due to the small number of host rhyodacite phenocrysts included in the study and because both crystals analyzed produced values similar to the host whole rock isotopic values. However, petrographic evidence does show evidence for crystal transfer from mafic inclusions into the host rhyodacite. Additional isotopic analyses would likely show crystals in the host rhyodacite with internal isotopic contrast.

Profile measurement and analysis

We analyzed three samples from dome B to assess variability in shared characteristics between mafic inclusion and host rhyodacite samples. Polished thin sections are analyzed on a JEOL 733 Superprobe with backscatter electron detector and four wavelength dispersive X-ray spectrometers (WDS). 1,000×1,000 pixel backscatter electron images (BSE) are collected with a 15keV accelerating potential, 15nA beam current, and a 1 μm beam diameter to maximize image contrast and spatial resolution. WDS calibration points are collected with an 8–10nA accelerating potential and 5 μm spot size to minimize Na mobilization. Seven to twelve BSE images of each crystal are averaged to improve the signal-to-detector noise ratio (Fig. 6) (Ginibre et al. 2002). Profiles are measured from WDS-calibrated BSE images using established techniques (Tribold 2003). Profiles are measured along the shortest distance from core to rim where possible. Other profile orientations are measured if they have equivalent zone spacing and provide more detailed resolution of the zoning pattern. This is often necessary to avoid fractures or in broken crystals. Cracks significantly degrade profile correlation if included in zoning profiles because they produce negative compositional anomalies that are often larger than anorthite variations. Profiles are collected in segments to avoid fractures and reconstructed in an electronic spreadsheet.

SCD and profile normalization use correlation window widths and significance levels determined for each sample (Fig. 7). Correlation window widths are set to 40 points in host phenocrysts and 30 points in mafic inclusion profiles as a balance between short profiles in microlites and matching the length scale of zoning features. Varying the correlation window width between 10 and 80 points does not significantly change SCD results. Normalization is set to a stretching range of 0.2–4.5 in 0.005 steps providing 861 potential best fits for each profile pairing. Internal consistency is checked in reciprocal plots of best-fit alignments (Fig. 8).

Application of SCD to $^{87}Sr/^{86}Sr$ in plagioclase

$^{87}Sr/^{86}Sr$ data provide an opportunity to assess the correspondence between chemical tracers in the same phase (Fig. 9). Tepley et al. (1999) aligns $^{87}Sr/^{86}Sr$ profiles to a common length, which must be compensated for prior to SCD construction (Wallace and Bergantz 2004). First, 15 points are interpolated between each microdrill point to provide adequate resolution for the empirical alignment routine. The addition of extra points may not represent the actual variation between microdrill points, but provides a first-order approximation consistent with available measurements. Profiles are then normalized over an interval 0.2–2.5 at a 0.005 step size with a correlation threshold of 0.5 to find the best fit. Comparison to the anorthite profiles presented in this paper must be considered with caution because they are not measured from the same crystals. However, the $^{87}Sr/^{86}Sr$ data offer low analytical uncertainty and while detailed comparison of profiles is not warranted, first-order comparisons of the behavior of plagioclase solid solution and $^{87}Sr/^{86}Sr$ are reasonable within reasonable assumptions of spatial uncertainty and the representatives of each population.

The resolution of the interpolated $^{87}Sr/^{86}Sr$ profiles is lower than anorthite profiles from the calibrated BSE images complicating comparison. The consistency of the comparison of $^{87}Sr/^{86}Sr$ and anorthite SCD is tested by reducing the resolution of a subset of anorthite profiles to match the $^{87}Sr/^{86}Sr$ profiles and then correlating them under the same conditions.

Results from shared characteristic diagrams of Chaos Crags plagioclase

Data quality

SCD analyses show narrow intervals of shared characteristics between crystals in the host rhyodacite and inclusion populations (Fig. 8). Most decorrelation points are near profile rims. Decorrelation near crystal rims is due to either a narrow interval of shared characteristics, or decorrelation at the apparent core when a profile has been measured from an off-center section (Fig. 6). This can be attributed to: good alignment and correlation to the core, poor alignment, or the variable profile recording a small portion of the reference zoning profile. The first profile in the alignment process is the shortest, so it is taken as a best fit by default when the decorrelation point never migrates away from the rim of the crystal. Where profiles are smooth, as in most microlite profiles, there is less information for the algorithm to constrain a best fit. Short profiles will preferentially decorrelate near the rim because correlation window widths need to be large in order to overlap zoning features and not be sensitive to smaller scale changes.

The internal consistency of profile normalization is checked in reciprocal plots (Fig. 8). Most alignments plot within error of the reciprocal line, with about 30% of pairings too long or short. Interpolation to long stretchings relative to measured lengths causes low-variance portions of profiles to become nearly flat. If variance within the correlation window is sufficiently reduced by interpolation, correlation coefficients will converge on zero, potentially controlling the position of the decorrelation point. This systematically skews decorrelation points toward crystal rims, producing an asymmetry in profile normalization best-fit alignments between reference-variable pairs. Reducing the stretching range limits interpolation bias for those crystal pairs and usually improves alignment quality. Alignments that plot below the reciprocal line often form linear arrays along the shortest stretching. The linear arrays are created by decorrelations within a window width of the rim in reference, but not variable profiles. These profile pairs have little to no shared characteristics within the resolution of the cross-correlation profile.

Trends in shared characteristic diagrams

Most decorrelation points in host rhyodacite sample L02-036 are located near crystal rims, at the first or second resorption zone (Fig. 7a) (Table 1). SCD from sample L02-018 are more heterogeneous than L02-036 (Fig. 7b). Decorrelation points are closer to the rim and few profiles correlate beyond the first resorption zone. Many crystals decorrelate at the first point in profiles, indicating that rims have different zoning patterns and would not correlate well at any alignment. These profile comparisons plot as points in a cluster near the origin in reciprocal plots (Fig. 8). When profiles do not correlate at the rim, the algorithm selects the first point in the interpolation matrix. This generates the linear arrays of points parallel to plot axes with large error bars due to the increased proportion of the correlative profile accounted by the correlation window.

Decorrelation points in inclusion sample L02-034 cluster close to the rim in both phenocryst and microlite populations and have fewer shared characteristics than either of the host rhyodacite samples (Fig. 7c). Profiles one through three decorrelate at the inside edge of the high-Ca rim on phenocrysts. Profiles from the same phenocryst in mafic inclusions do not correlate beyond rim zones due to sieve textures. Microlites correlate well within the spatial uncertainty of the correlation window. No detectable shared characteristics are observed in plagioclase from mafic inclusions beyond outer high-Ca rims, and microlite populations.

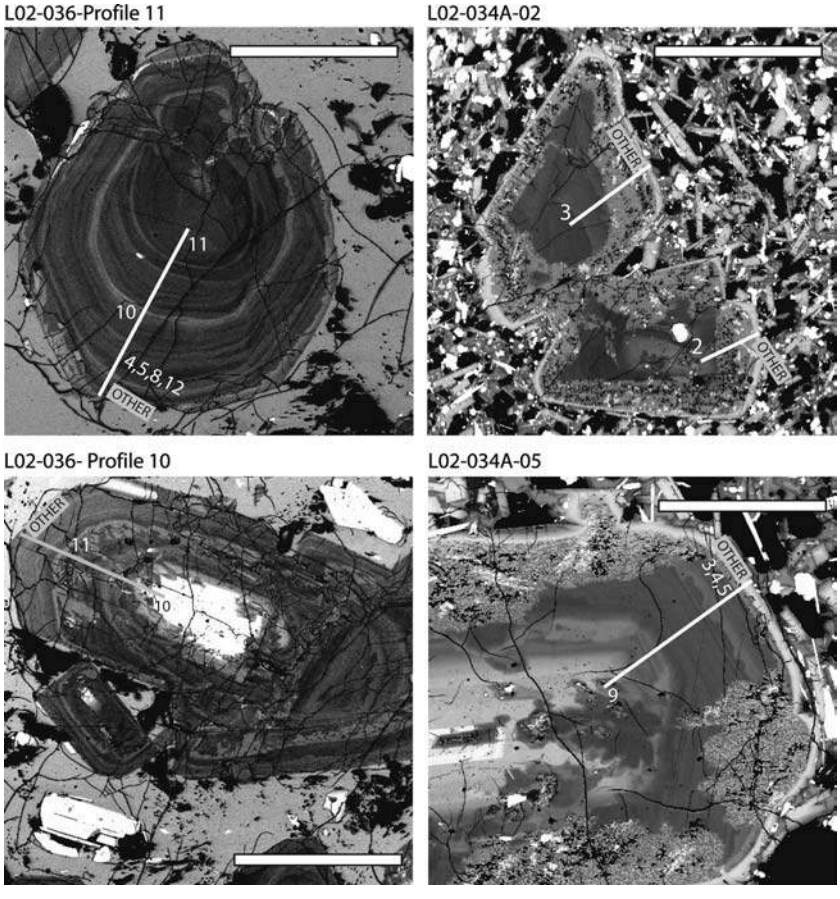

Fig. 6 Decorrelation points plotted on BSE images. Most decorrelation points cluster at the first spike in anorthite content. Scale bars are 1mm long. Anorthite content in BSE images of plagioclase is linearly correlated with grayscale. Brighter grayscale values reflect higher anorthite contents. Image labels match profile indices in Fig. 7. Zoning textures are similar in phenocrysts from host rhyodacite samples L02-036 and L02-018. Phenocrysts from L02-034 have substantial sieve texturing surrounded by normally zoned rims correlative with microlites zoning patterns. Samples L02-034 and L02-036 are from the same outcrop (location shown in Fig. 2)

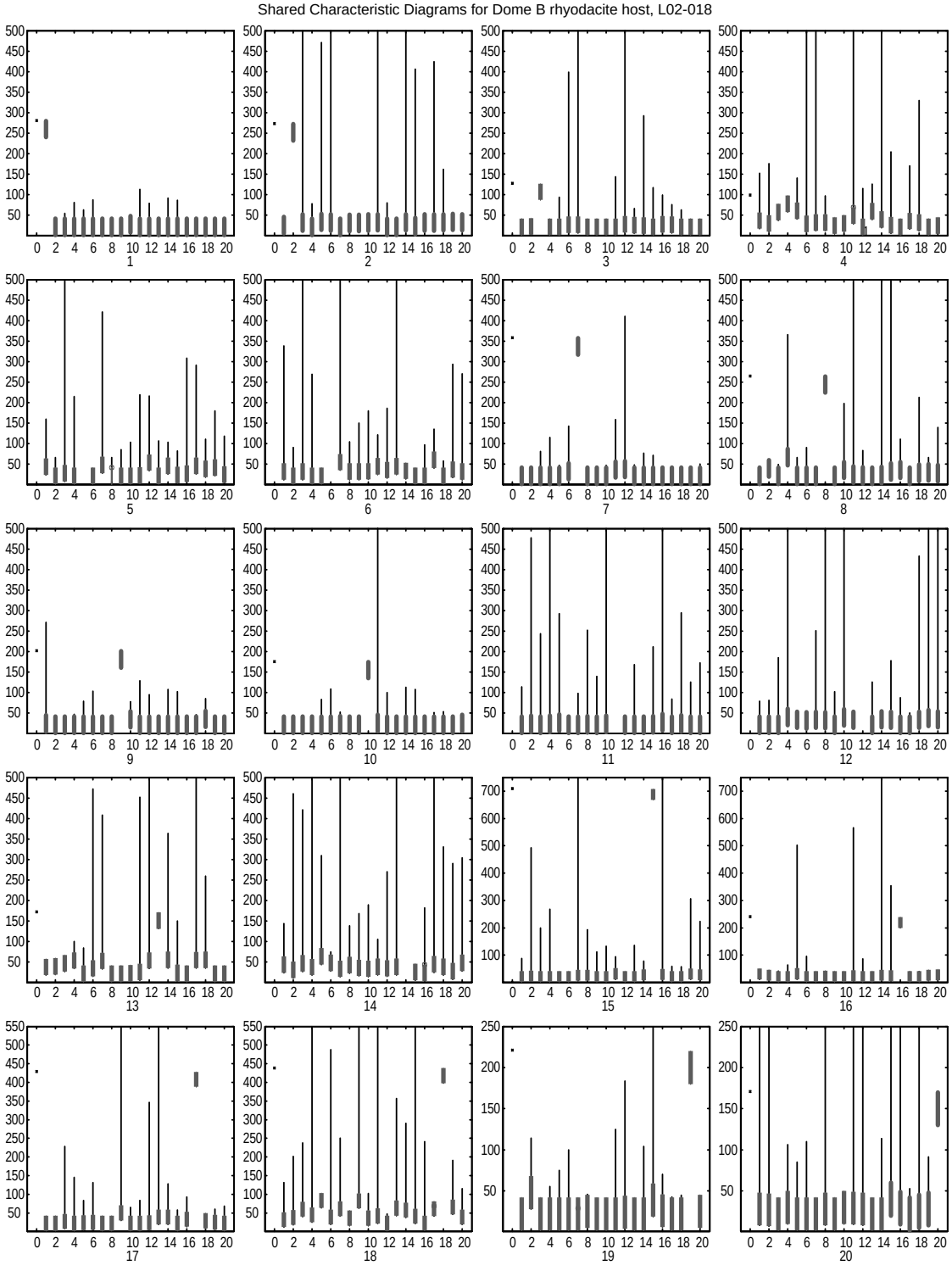

Fig. 7 Shared characteristic diagrams (SCD) for plagioclase from dome B. Each box is a SCD for a reference profile against all variable profiles, as discussed in text and Fig. 5. The reference profile number is given below each plot and the index of each profile is given along the *x*-axis. The length of the reference profile is indicated by a point at the left side of the plot. The *wide gray lines* are the position and spatial uncertainty of the decorrelation point along the profile. The *thin black line* represents the non-correlative segment of the zoning profile. The *blank area* between the *wide gray line* and the rim is the correlative segment of the profile. **a** Sample L02-018, host rhyodacite. **b** Sample L02-036, host rhyodacite. **c** L02-034, mafic inclusion co-located with sample L02-036

SCD for $^{87}Sr/^{86}Sr$ data have large intervals of shared characteristics with decorrelation points plotting near crystal cores (Fig. 9). The majority of profile alignments are reciprocal within alignment uncertainty indicating that profile alignments are internally consistent. The narrow range of reciprocal plots is consistent with

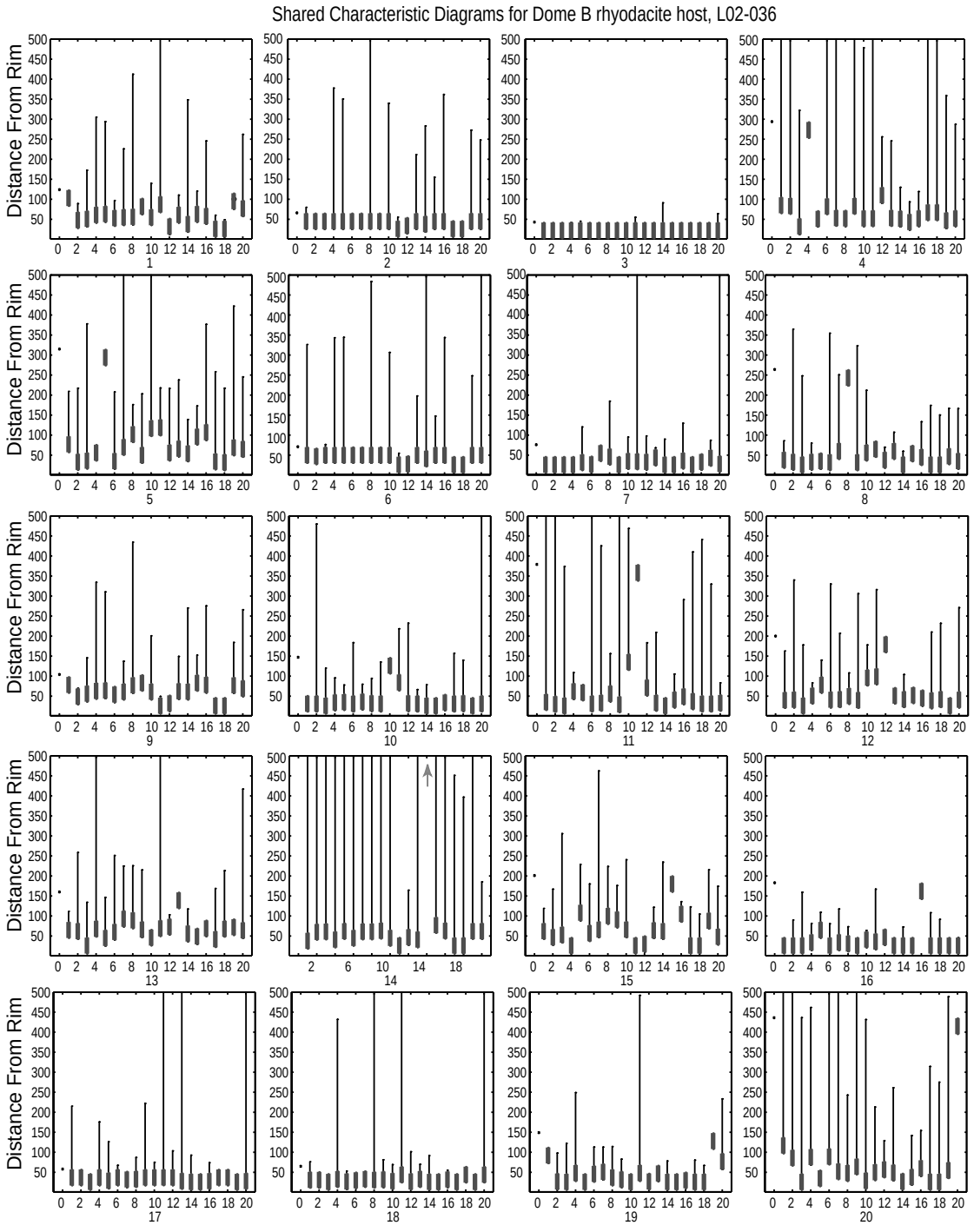

Fig. 7 (Contd.)

selection of aligned and on-center sections. Profile two consistently decorrelates near the second microdrill point, where $^{87}Sr/^{86}Sr$ values spike to more radiogenic values. Profile normalization points above the reciprocal line reflect interpolation bias between microdrill points with similar $^{87}Sr/^{86}Sr$ values (Fig. 8).

The reduced resolution anorthite profile data set used to test the reliability of the comparison between $^{87}Sr/^{86}Sr$ and anorthite profiles showed similar results to the full resolution anorthite data. The SCD from the reduced resolution anorthite data set did show more shared history than the full resolution data set, but the difference between the anorthite and $^{87}Sr/^{86}Sr$ data set is considerably greater. The comparison between these SCD data sets should be regarded as illustrative of the differences in data content, but fundamentally qualitative due to spatial uncertainties arising from the data manipulation.

Fig. 7 (Contd.)

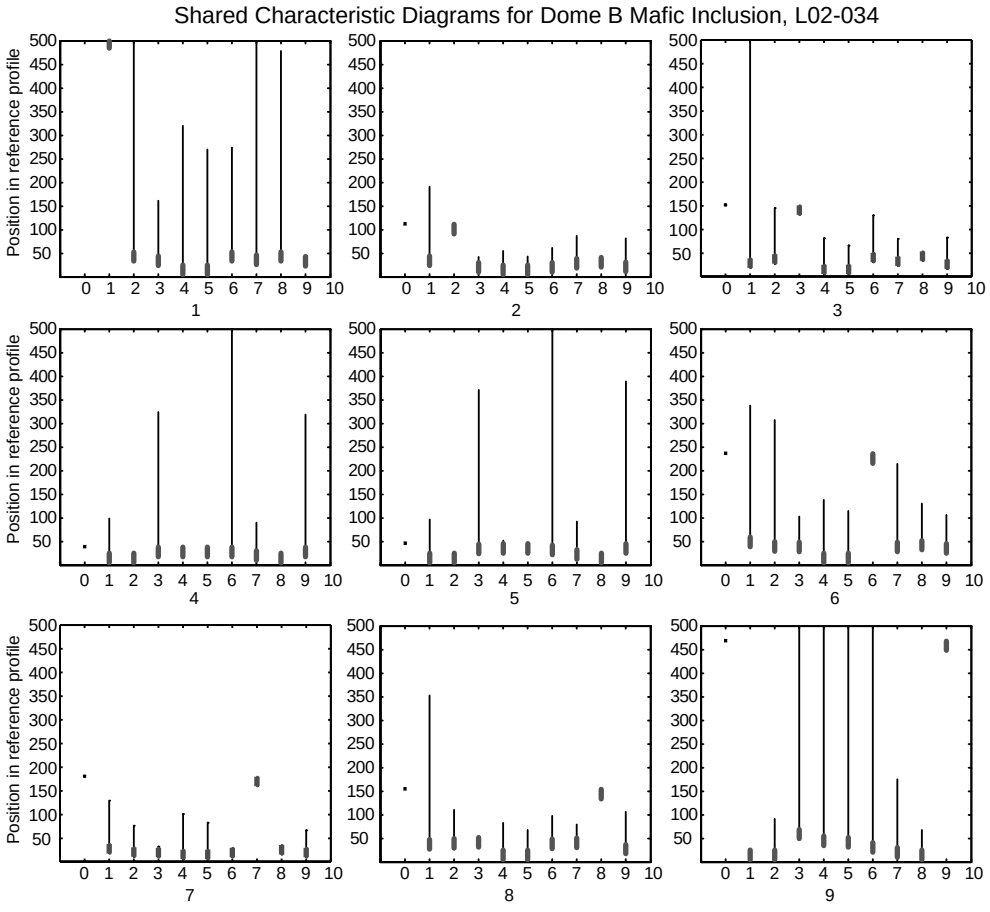

Discussion

The distribution of shared characteristics in anorthite profiles show decreasing shared history from host rhyodacite to mafic inclusions. Using shared characteristics as a proxy for shared history, this implies less shared history in plagioclase populations from mafic inclusions. The difference in shared history between inclusion and host samples is a result of the gathering of diverse crystal populations into a common environment during crystal transfer. Additionally, the commingling environment is heterogeneous and temporally variable in the activity of water, composition, and temperature. Constraining the intensive controls on plagioclase composition and their relationship to SCD provide a window into the commingling and crystal transfer processes.

Plagioclase composition is dependent on temperature, melt composition, activity of water, and pressure (Yoder 1957; Housch 1991; Pearce 1994). Crystallization and decompression during ascent will produce normal zoning patterns consistent with zoning textures in microlites (Fig. 6) (Cashman 1992; Blundy and Cashman 2001). Correlation in microphenocrysts indicates similar histories. However, decreases in pressure will not produce the Type II zoning features observed in phenocrysts. Thus, while decompression may be a controlling factor in microlite populations, simple decompression is not responsible for the heterogeneity in phenocryst populations. Increases in temperature and water content produce higher anorthite contents in plagioclase. Experimental studies of plagioclase dissolution show that albitic plagioclase heated in a calcic melt produce sieve textures, while heating in a felsic melt will produce simple dissolution (Tsuchiyama 1985). This is consistent with the observation of sieve-textured phenocrysts in mafic inclusions and dissolution in the host rhyodacite. The vesicularity and chilled margins of mafic inclusions suggest that they are a source of both heat and volatiles (Eichelberger 1980; Heiken and Eichelberger 1980). Because water and temperature have similar effects on plagioclase composition, their effects are not separable using plagioclase composition alone. Thus, either temperature or volatiles could produce the observed zoning textures in phenocryst populations. Diffusion at mafic–felsic contacts and commingling will produce heterogeneous environments characterized by gradients across inclusions and within the host rhyodacite, consistent with the heterogeneity observed in SCD.

Whole rock analyses of $^{87}Sr/^{86}Sr$ and major elements are separated by a broad compositional gap

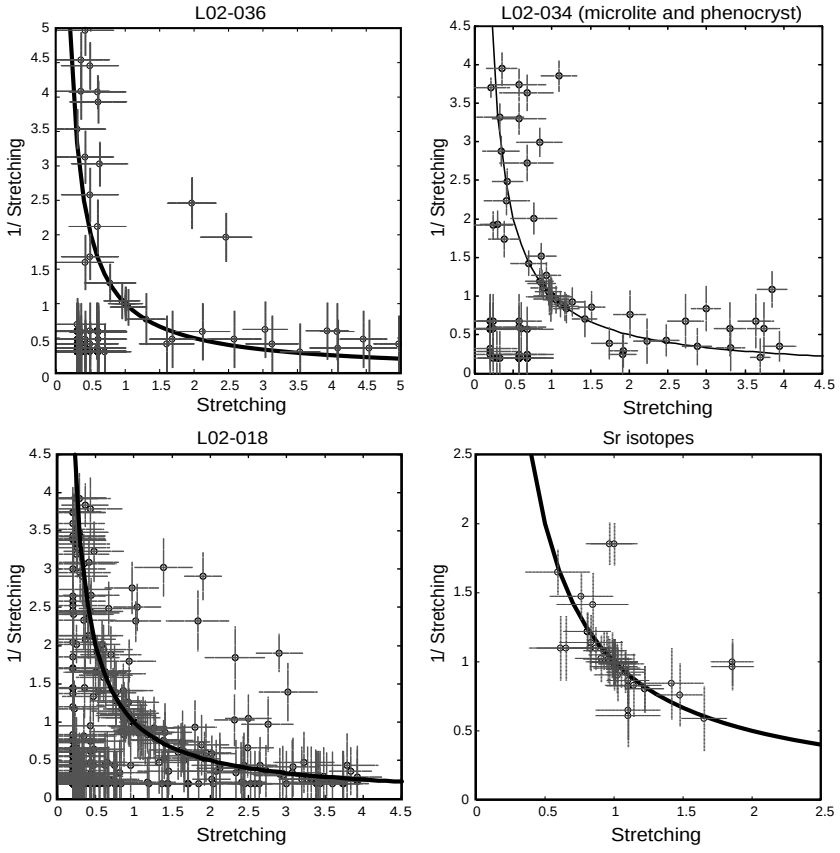

Fig. 8 Reciprocal plots of best-fit profile alignments. The best-fit stretching for each reference–variable profile pair should be reciprocal and plot on a $1/x$ line. A stretching of 2.0 should have a reciprocal stretching of 0.5 when variable and reference profile classifications are swapped. Profiles that decorrelate near the rim have a larger uncertainty in alignment because changes in stretching have a larger impact in position closer to the core. Profile pairs that plot below the *gray line* align at too short a stretching, as discussed in text

between mafic inclusions and host rhyodacites, forming clusters along a binary mixing line defining end-member compositions (Tepley et al. 1999). Cooling and crystallization in isolated mafic inclusions change melt composition producing normal zoning in plagioclase. Similar microphenocryst core and phenocryst rim compositions indicate phenocryst transfer into mafic inclusions early in microlite growth history. Isotopic values are not a function of pressure, temperature or water content and reflect only the melt composition at the time of crystallization. Thus, we submit that $^{87}Sr/^{86}Sr$ in inclusion phenocrysts are a good index of composition during crystal transfer. Decorrelation points in SCD of $^{87}Sr/^{86}Sr$ are dominantly near crystal cores indicating shared history. This observation is inconsistent with the observation of little to no shared history in anorthite profiles. If composition has more shared history than another chemical tracer in the same phase sensitive to composition, temperature, and water content, then temperature and/or activity of water exert stronger control on heterogeneity. This implies that the composition of the part of the Chaos Crags magma system involved in the eruption is less variable than the thermal or activity of water. This conceptualization of heterogeneity is similar to quantitative measures based on characteristic homogeneous length scales (Danckwerts 1952; Oldenburg et al. 1989).

The difference in SCD between anorthite profiles in the host rhyodacite and mafic inclusions indicate that the crystal transfer process produces more heterogeneous crystal populations. If the control on heterogeneity is a combination of temperature and volatile content effects, then the crystal transfer process must be associated with a thermally heterogeneous environment or draw phenocrysts from diverse sources. Regardless, if the heterogeneity of the host crystal population is used as a baseline, crystal transfer into a mafic magma increases the heterogeneity of the transferred crystal population. Differences between host samples L02-018 and L02-036 SCD demonstrate that crystal populations from different parts of a single flow may have differences in shared history. If L02-018 was erupted after L02-036, the decrease in shared history may represent an increase in the degree of commingling of the host rhyodacite during convection of the Chaos Crags magma chamber.

The protracted history recorded in individual phenocrysts as multiple resorption surfaces and differing degrees of shared history lead to two important conclusions about the Chaos Crags system: (1) many of the crystals have seen several cycles of resorption and growth prior to the eruption of the Chaos Crags lavas indicating that many of the phenocrysts are antecrystic; and (2) adjacent crystals in a thin section with similar textures may have similar process history from the same or separate events and not have shared history sensu

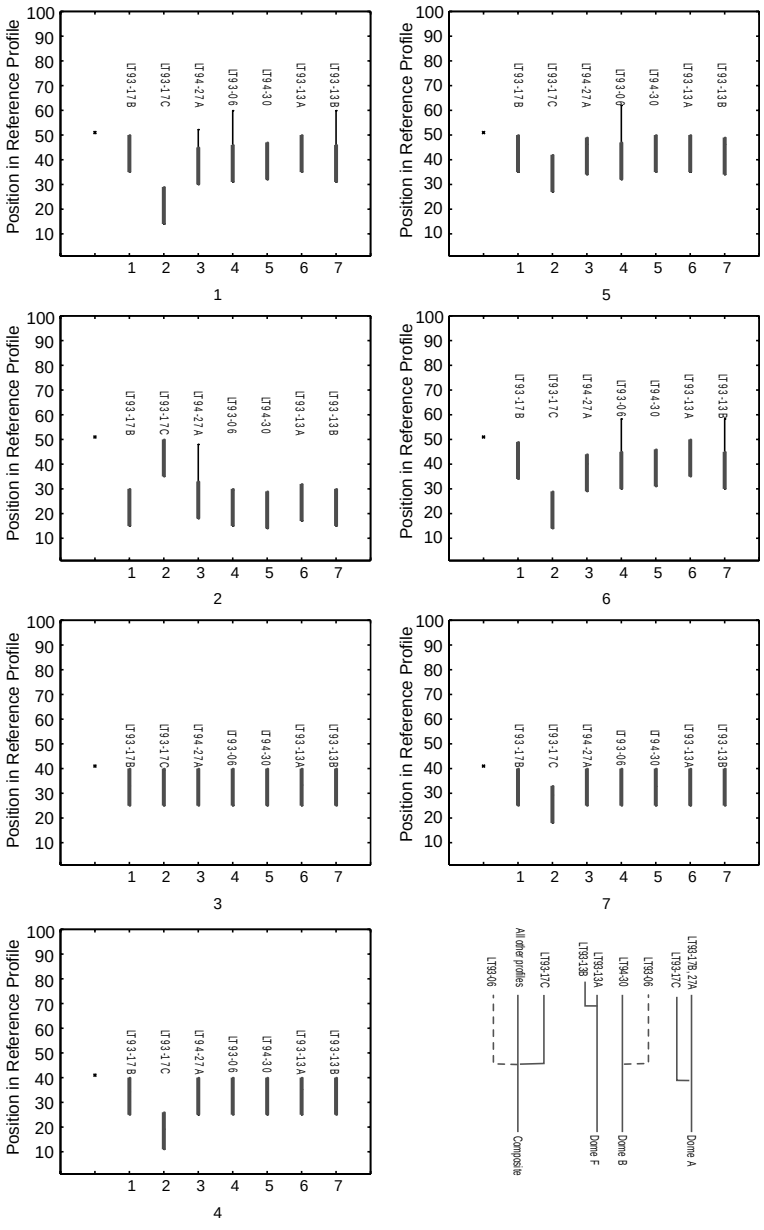

Fig. 9 Shared characteristic diagrams for $^{87}Sr/^{86}Sr$ profiles in plagioclase from mafic inclusions. SCD are created by interpolating published profiles (Tepley et al. 1999) to 60 points and applying the empirical profile normalization technique with a correlation threshold of 0.5 and correlation window size of 15 points. SCD results do not significantly change with window widths set to10 or 20 points. Reciprocal plots generally show good internal consistency within error. The narrow range of profile normalization best fits indicates that crystals are similarly aligned in thin section relative to cores and growth zones. Phylogeny diagrams for the SCD data are presented in the lower right corner. Decorrelation points in SCD are represented as branching points in the phylogeny. For example, profiles 1 and 2 (LT93-17B and LT93-17C) decorrelate about halfway along the profile producing a branching in the phylogeny in dome A representing a divergence in their shared history. A dashed line is used in the phylogeny where shared history is uncertain

stricto. However, the evaluation of shared history is dependent on the chemical tracer analyzed in the zoning study. Comparison of SCD may help separate true antecrysts from crystal populations that have grown in heterogeneous environments. Differences in SCD between crystals may be the equivalent of finding zircons of different ages in a crystal population.

Table 1 Sample locations and lithology. Sample locations are shown in Fig. 2

Sample	UTM	Dome	Sample lithology
L02-018	10T 0625934, 4485730	Dome B	Rhyodacite host
L02-034	10T 0624490, 4486850	Dome B	Mafic inclusion
L02-036	10T 0624490, 4486850	Dome B	Rhyodacite host

Conclusions

In general, SCDs provide a framework for mutual interpretation of diverse data types. This facilitates assessment and ranking of relative heterogeneity of defined chemical tracers and phases in magmatic systems. While we apply SCD to plagioclase, SCD are applicable to other zoned phases and chemical tracers. This flexibility increases the utility of existing data sets and provides a consistent framework for crystal selection for expensive and time-consuming analytical techniques. SCD provide previously unavailable constraints on the distribution and relative heterogeneity of specific chemical tracers in magmatic systems. A particularly exciting possibility is the application of SCD to ages determined

by spot analyses in accessory phases such as zircon and allanite coupled with REE and major element analyses (Vazquez and Reid 2001, 2002). SCD of crystal zoning data from mineral separates can also provide constraints on the pre-eruptive distribution of heterogeneity of key elements such as Ra, Ba, Th, and other REE critical for assessment of residence times in magmatic systems (Cooper and Reid 2003; Turner et al. 2003).

At Chaos Crags, the observation of less variation in $^{87}Sr/^{86}Sr$ SCD than in anorthite profile SCD is consistent with a system in which the melt in the mafic and felsic reservoirs are compositionally homogeneous prior to commingling, while the temperature and volatile contents are more variable. The results of this study are consistent with reasonable expectations for a small volume commingled system, indicating that application of SCD to data from other systems is promising.

Acknowledgements We would like to thank M. Clynne for a preprint of the Lassen Peak geologic map, and introduction to the area. M. Clynne and M. Reagan provided detailed and thoughtful reviews that improved the content and presentation of this manuscript. K. Cooper provided an additional review, which was also helpful in improving this manuscript. This research is funded by NSF grants EAR-9805336 and EAR-0106441.

References

Allegre CJ, Jaupart C (1981) Oscillatory zoning: a pathological case of crystal growth. Nature 294:223–228

Anderson AT Jr (1983) Oscillatory zoning of plagioclase: Nomarski interference contrast microscopy of etched sections. Am Miner 68:125–129

Bacon CR, Druitt TH (1988) Compositional evolution of the zoned calcalkaline magma chamber of Mount Mazama, Crater Lake, Oregon. Contrib Mineral Petrol 98:224–256

Bergantz GW, Breidenthal RE (2001) Non-stationary entrainment and tunneling eruptions: a dynamic link between eruption processes and magma mixing. Geophys Res Lett 28(16):3075–3078

Blundy J, Cashman K (2001) Ascent-driven crystallisation of dacite magmas at Mount St Helens, 1980–1986. Contrib Mineral Petrol 140(6):631–650

Blundy J, Wood B (2003) Partitioning of trace elements between crystals and melts. Earth Planet Sci Lett 210(3–4):383–397

Bottinga Y, Kudo A, Weill D (1966) Some observations on oscillatory zoning and crystallization of magmatic plagioclase. Am Miner 51:792–806

Cashman KV (1992) Groundmass crystallization of Mount St Helens dacite, 1980–1986—a tool for interpreting shallow magmatic processes. Contrib Mineral Petrol 109(4):431–449

Christiansen RL, Clynne MA, et al. (2002) Geologic map of the Lassen Peak, Chaos Crags, and Upper Hat Creek area, California. US Geological Survey Geologic Investigations Series I-2723.

Clynne MA (1999) A complex magma mixing origin for rocks erupted in 1915, Lassen Peak, California. J Petrol 40(1):105–132

Clynne MA, Christiansen RL, et al. (2002) Radiocarbon dates from volcanic deposits of the Chaos Crags and cinder cone eruptive sequences and other deposits, Lassen Volcanic National Park and vicinity, California. U.S. Geological Society Open-File Report 02–290, 21p.

Clynne MA, Muffler LJP (1989) Lassen Volcanic National Park and vicinity. In: Chapin CE, Zidek J (eds) Field excursions to volcanic terranes in the western United States, vol II, Cascades and Intermountain West, New Mexico Bureau of Mines and Mineral Resources Memoir 47, pp183–194

Cooper KM, Reid MR (2003) Re-examination of crystal ages in recent Mount St. Helens lavas: implications for magma reservoir processes. Earth Planet Sci Lett 213(1–2):149–167

Costa F, Chakraborty S, et al. (2003) Diffusion coupling between trace and major elements and a model for calculation of magma residence times using plagioclase. Geochim Cosmochim Acta 67(12):2189–2200

Danckwerts PV (1952) The definition and measurement of some characteristics of mixtures. Appl Sci Res A3:279–296

Davidson JP, Tepley FJ III (1997) Recharge in volcanic systems: evidence from isotope profiles of phenocrysts. Science 275:826–829

Davidson J, Tepley F III, et al. (2001) Magma recharge, contamination and residence times revealed by in situ laser ablation analysis of feldspar in volcanic rocks. Earth Planet Sci Lett 184:427–442

Druitt TH, Bacon CR (1989) Petrology of the zoned calcalkaline magma chamber of Mount Mazama, Crate Lake, Oregon. Contrib Mineral Petrol 101:245–259

Eichelberger JC (1980) Vesiculation of mafic magma during replenishment of silicic magma reservoirs. Nature 288(5790):446–450

Eichelberger JC, Chertkoff DG, et al. (2000) Magmas in collision: rethinking chemical zonation in silicic magmas. Geology 28(7):603–606

Fowler A, Prokoph A, et al. (2002) Organization of oscillatory zoning in zircon: analysis, scaling, geochemistry, and model of a zircon from Kipawa, Quebec, Canada. Geochim Cosmochim Acta 66(2):311–328

Ginibre C, Kronz A, et al. (2002) High-resolution quantitative imaging of plagioclase composition using accumulated backscattered electron images: new constraints on oscillatory zoning. Contrib Mineral Petrol 142(4):436–448

Greenwood H, McTaggert K (1957) Correlation of zones in plagioclase. Am J Sci 255:656–666

Hart GL, Johnson CM, et al. (2002) Osmium isotope constraints on lower crustal recycling and pluton preservation at Lassen Volcanic Center, CA. Earth Planet Sci Lett 199(3–4):269–285

Heiken G, Eichelberger JC (1980) Eruptions at Chaos Crags, Lassen Volcanic National Park, California. J Volcan Geotherm Res 7(3–4):443–481

Izbekov PE, Eichelberger JC, et al. (2002) Calcic cores of plagioclase phenocrysts in andesite from Karymsky volcano: evidence for rapid introduction by basaltic replenishment. Geology 30(9):799–802

Lheureux I, Fowler AD (1996) Isothermal constitutive undercooling as a model for oscillatory zoning in plagioclase. Can Miner 34:1137–1147

Murphy MD, Sparks RSJ, et al. (2000) Remobilization of andesite magma by intrusion of mafic magma at the Soufriere Hills Volcano, Montserrat, West Indies. J Petrol 41(1):21–42

Oldenburg CM, Spera FJ, et al. (1989) Dynamic mixing in magma bodies: theory, simulations and implications. J Geophys Res 94:9215–9236

Pearce TH (1984) The analysis of zoning in magmatic crystals with emphasis on olivine. Contrib Mineral Petrol 86:149–154

Pearce TH (1994) Recent work on oscillatory zoning in plagioclase. In: Parsons I (ed) Feldspars and their reactions, vol 421. Kluwer Academic, London, pp 313–350

Pearce T, Kolisnik A (1990) Observations of plagioclase zoning using interference imaging. Earth Sci Rev 29:9–26

Pietruszka AJ, Garcia MO (1999) The size and shape of Kilauea Volcano's summit magma storage reservoir: a geochemical probe. Earth Planet Sci Lett 167(3–4):311–320

Reagan MK, Sims KW, et al. (2003) Timescales of differentiation from mafic parents to rhyolite in North American continental arcs. J Petrol 44 (9):1703–1726

Seaman SJ, Wobus RA, et al. (1995) Volcanic expression of bimodal magmatism—the Cranberry Island Cadillac Mountain Complex, Coastal Maine. J Geol 103(3):301–311

Tepley FJ III, Davidson JP, et al. (1999) Magmatic interactions as recorded in plagioclase phenocrysts of Chaos Crags, Lassen volcanic center, California. J Petrol 40:787–806

Tepley FJ III, Davidson JP, et al. (2000) Magma mixing, recharge and eruption histories recorded in plagioclase phenocrysts from El Chichon Volcano, Mexico. J Petrol 41(6):1397–1411

Tobisch OT., R. H. Vernon, et al. (1995) Polygenetic microgranitoid enclave swarms in granitic rocks, central Sierra Nevada, California. U.S. Geological Survey Circular 1129

Tollstrup DL, Ramos FC, et al. (2002) Short timescales for crustal residence, transport and contamination of flood basalt magma: crystal isotope stratigraphy of the Columbia River Basalt Group. Eos Trans AGU 83(47):V72D-01

Tribold S (2003) Feldspar zonation, magma chamber dynamics, and the evolution of the Teide-Pico Viejo magmatic system. Geowissenshaftlichen Zentrum. Gottingen, Germany, Georg-August Universitat zu Gottingen:646

Troll VR, Schmincke HU (2002) Magma mixing and crustal recycling recorded in ternary feldspar from compositionally zoned peralkaline Ignimbrite 'A', Gran Canaria, Canary Islands. J Petrol 43(2):243–270

Tsuchiyama A (1985) Dissolution kinetics of plagioclase in the melt of the system diopside-albite-anorthite, and the origin of dusty plagioclase in andesites. Contrib Mineral Petrol 89:1–16

Turner S, George R, et al. (2003) Case studies of plagioclase growth and residence times in island arc lavas from Tonga and the Lesser Antilles, and a model to reconcile discordant age information. Earth Planet Sci Lett 214(1–2):279–294

Vance JA (1962) Zoning of igneous plagioclases: normal and oscillatory zoning. Am J Sci 260:746–760

Vazquez JA, Reid MR (2001) Timescales of magmatic evolution by coupling core-to-rim 238U-230Th ages and chemical compositions of mineral zoning in allanite from the youngest Toba Tuff. Eos Trans AGU 82(47):F1350

Vazquez JA, Reid MR (2002) Constraining the timing of magmatic evolution in the Youngest Toba Tuff rhyolite through dating of zoning in allanite 2002. Twelfth Annual V.M. Goldschmidt Conference. Geochim Cosmochim Acta 66(15A):A802

Waight T, Maas R, et al. (2000) Fingerprinting feldspar phenocrysts using crystal isotopic composition stratigraphy: implications for crystal transfer and magma mingling in S-type granites. Contrib Mineral Petrol 139:227–239

Waight TE, Wiebe RA, et al. (2001) Isotopic responses to basaltic injections into silicic magma chambers: a whole-rock and microsampling study of macrorhythmic units in the Pleasant Bay layered gabbro–diorite complex, Maine USA. Contrib Mineral Petrol 142:323–335

Wallace GS, Bergantz GW (2002) Wavelet-based correlation (WBC) of crystal populations and magma mixing. Earth Planet Sci Lett 202:133–145

Wallace GS, Bergantz GW (2004) Constraints on mingling of crystal populations from off-center zoning profiles: a statistical approach. Am Miner 89(2):64–73

Wiebe RA, Smith D, et al. (1997) Enclaves in the Cadillac Mountain granite (coastal Maine): samples of hybrid magma from the base of the chamber. J Petrol 38(3):393–423

Williams H (1928) A recent eruption near Lassen Peak, California. Univ CA Publ Geol Sci 17(7):241–263

Williams H (1931) The dacites of Lassen Peak and vicinity, California, and their basic inclusions. Am J Sci 22:385–403

Wolff JA, Ramos FC, et al. (1999) Sr isotope disequilibrium during differentiation of the Bandelier Tuff: constraints on the crystallization of a large rhyolitic magma chamber. Geology 27(6):495–498